

## Iron meteorites and their weathering products: high velocity resolution Mössbauer spectroscopy of the iron-bearing minerals

MIKHAIL V. GORYUNOV<sup>1,2</sup>, GRIGORIY A. YAKOVLEV<sup>1</sup>, ANDREI V. CHUKIN<sup>3</sup>, VICTOR I. GROKHOVSKY<sup>1</sup>,  
VLADIMIR A. SEMIONKIN<sup>1,2</sup> and MICHAEL I. OSHTRAKH<sup>1,2,\*</sup>

<sup>1</sup> Department of Physical Techniques and Devices for Quality Control, Institute of Physics and Technology, Ural Federal University, Ekaterinburg 620002, Russian Federation

<sup>2</sup> Department of Experimental Physics, Institute of Physics and Technology, Ural Federal University, Ekaterinburg 620002, Russian Federation

\*Corresponding author, e-mail: oshtrakh@gmail.com

<sup>3</sup> Department of Theoretical Physics and Applied Mathematics, Institute of Physics and Technology, Ural Federal University, Ekaterinburg 620002, Russian Federation

**Abstract:** The iron meteorites Anyujskij IIAB, Sikhote-Alin IIAB, Sterlitamak IIIAB, Aliskerovo IIIE-an and Dronino iron-ung and products of Dronino meteorite weathering in clay sand were studied using Mössbauer spectroscopy with a high velocity resolution. Components revealed in the complex Mössbauer spectra were related to corresponding iron-bearing minerals. A difference in the oxidation products of two Dronino fragments was observed. The presence of siderite was found in the external surface oxidation layer in the second fragment, which may be a result of goethite bioreduction in clay sand.

**Key-words:** iron meteorites, weathering,  $\alpha$ -Fe(Ni,Co),  $\alpha_2$ -Fe(Ni,Co) and  $\gamma$ -Fe(Ni,Co) phases, magnetite, maghemite and goethite, siderite, Mössbauer spectroscopy.

### Introduction

Iron meteorites belong to differentiated meteorites and are classified as magmatic and nonmagmatic groups and ungrouped meteorites (Rubin, 1997). Iron meteorites consist of Fe-Ni-Co alloy as a matrix with minor inclusions of iron-nickel phosphides, sulfides and some other mineral exsolutions. The main minerals of the matrix are b.c.c.  $\alpha$ -Fe(Ni,Co) phase, b.c.c.  $\alpha_2$ -Fe(Ni,Co) phase, f.c.c.  $\gamma$ -Fe(Ni,Co) phase and ordered f.c.c.  $\gamma$ -FeNi phase. Iron-nickel phosphide (Fe, Ni)<sub>3</sub>P, schreibersite, occurs in the form of massive inclusions and/or prismatic microcrystals ('rhabdites') precipitated in  $\alpha$ -Fe(Ni,Co) matrix. Troilite FeS inclusions in  $\alpha$ -Fe(Ni,Co) matrix can contain small amount of daubréelite, FeCr<sub>2</sub>S<sub>4</sub>. These minerals were formed in the space extreme conditions, for instance, with a cooling rate of 1–15° per million years in the  $\gamma$ - $\alpha$  transformation interval. Moreover, these minerals might be affected by meteoroids or their parent bodies' collisions and shock reheating. Therefore, these minerals have some structural features different from their terrestrial analogues. Detailed features and mineral composition of iron meteorites can be found, for instance, in reviews by Buchwald (1975), Rubin (1997), Goldstein *et al.* (2009) and Grady *et al.* (2014). The terrestrial history of iron meteorites is related in part to their

weathering processes. Meteoritic  $\alpha$ -Fe(Ni,Co),  $\alpha_2$ -Fe(Ni,Co) and  $\gamma$ -Fe(Ni,Co) oxidation processes as a result of interactions of water, oxygen and other chemicals with iron alloy can be also different from similar oxidation of terrestrial alloys. Therefore, investigation of meteoritic minerals in different meteorites and their weathering is of interest.

The <sup>57</sup>Fe Mössbauer spectroscopy is a useful technique to study iron-bearing minerals, including those in meteorites. This technique is the most sensitive to the <sup>57</sup>Fe hyperfine parameters which are sensitive to iron local microenvironment variations that cannot be detected by any other techniques. As far as iron meteorites demonstrate complicated composition of the Fe-Ni-Co alloys, with the presence of  $\alpha$ -Fe(Ni,Co),  $\alpha_2$ -Fe(Ni,Co),  $\gamma$ -Fe(Ni,Co) and  $\gamma$ -FeNi phases (besides inclusions) with variations in Ni and Co concentration within one phase, Mössbauer spectra of iron meteorites demonstrate a complex character related to the superimposition of several spectral components which cannot be easily distinguished using conventional Mössbauer spectroscopy. Therefore, Mössbauer spectroscopy with a high velocity resolution, which demonstrated additional possibilities in the detailed study of iron-bearing minerals in meteorites (see Grokhovsky *et al.*, 2008, 2009; Oshtrakh *et al.*, 2008; 2013a, 2015), was used for the investigation of

several iron meteorites from different groups (hexahedrites, octahedrites and ataxites) with different Ni concentration (see Goldstein *et al.*, 2009) and products of surface terrestrial weathering obtained from one of them.

## Materials and methods

Four magmatic iron meteorites Anyujskij IIAB, Sikhote-Alin IIAB (both are coarse octahedrites), Sterlitamak IIIAB and anomalous Aliskerovo IIIE-an (both are medium octahedrites) and one ungrouped iron meteorite Dronino iron-ung (probably an ataxite) were chosen for the study. Polished slices of iron meteorites fragments were analyzed using optical microscopy. Then powdered samples were prepared for X-ray diffraction (XRD) and Mössbauer spectroscopy. Due to the long terrestrial age of Dronino iron-ung meteorite, which was evaluated to more than 1000 years, the weathering processes of this meteorite were additionally investigated. For this purpose, the surface oxidation products from two Dronino fragments (No 1 and No 2) found in clay sand were extracted. The external and internal layers from fragment No 1 and the external layer from fragment No 2 were used. Additionally, samples from the external solid and internal friable layers of concretion found in clay sand surrounding Dronino fragment No 1 were taken also. Powdered samples of weathering products were studied using XRD and Mössbauer spectroscopy. For Mössbauer measurements all powdered samples were glued on iron-free aluminum foil with a sample thickness (surface iron density) of 6–8 mg Fe/cm<sup>2</sup>.

Metallographic analysis was carried out using an Axiovert 40 MAT microscope (Carl Zeiss). The XRD measurements of iron meteorites were done using XRD-7000 powder diffractometer (Shimadzu) operated at 40 kV and 30 mA with CuK<sub>α</sub> radiation using graphite monochromator. The scanning was performed in 2 $\Theta$  ranges from 40° to 120° with a step 0.05° and 15 s per step. The XRD study of weathering products was carried out using a PANalytical X'pert PRO diffractometer (The Netherlands) with CuK<sub>α</sub> radiation and position-sensitive X'Celerator detector with Ni filter. Measurements were done in 2 $\Theta$  ranges from 12° to 100° with a step of 0.03° and 200 s per step.

Mössbauer spectra measurements were carried out using an automated precision Mössbauer spectrometric system built on the base of the SM-2201 spectrometer with a saw-tooth shape velocity reference signal formed by the digital-analogue converter using quantification of 2<sup>12</sup> (with 4096 steps). This discretization of the velocity scale (velocity resolution) provides much better adjusting to resonance and significantly increases the quality of spectra measurements. This also increases the analytical possibilities of Mössbauer spectroscopy with extracting more reliable spectral components from the complex spectra. Detailed characteristics of this system were described elsewhere (Oshtrakh *et al.*, 2009; Semionkin

*et al.*, 2010; Oshtrakh & Semionkin, 2013). The 1.8×10<sup>9</sup> Bq <sup>57</sup>Co(Rh) source (Ritverc GmbH, St. Petersburg) was used at room temperature. The Mössbauer spectra were measured in transmission geometry with moving absorber in the cryostat at 295 K and recorded in 4096 channels. For their analysis, the spectra of Sikhote-Alin IIAB, Anyujskij IIAB, Aliskerovo IIIE-an and Sterlitamak IIIAB meteorites were converted into 1024 channels by a consequent summation of four neighboring channels, while the spectra of Dronino iron-ung meteorite and its weathering products were converted into 2048 channels by consequent summation of two neighboring channels to increase signal-to-noise ratio in these spectra. Statistics in the Mössbauer spectra converted into 1024 channels was in the range ~6.3 × 10<sup>5</sup>–87.3 × 10<sup>5</sup> counts per channel with a signal-to-noise ratio in the range 55–65 while that in the spectra converted into 2048 channels was in the range ~3.9 × 10<sup>5</sup>–2.6 × 10<sup>6</sup> counts per channel with a signal-to-noise ratio in the range 43–104. Each spectrum was measured during 1–2 weeks. Mössbauer spectra were fitted using the UNIVEM-MS program by the least squares procedure with a Lorentzian line shape (the line shape of the Mössbauer spectrum of the standard absorber of  $\alpha$ -Fe with a thickness of 7  $\mu$ m was purely Lorentzian with a line width of 0.236 ± 0.008 mm/s). The velocity resolution (velocity per one channel) was ~0.010 and ~0.020 mm/s per channel for the 2048 and 1024 channels Mössbauer spectra, respectively. The spectral parameters isomer shift,  $\delta$ , quadrupole splitting (quadrupole shift for magnetically split components),  $\Delta E_Q$ , magnetic hyperfine field,  $H_{\text{eff}}$ , line width,  $\Gamma$ , relative subspectrum area,  $A$ , and statistical quality of the fit,  $\chi^2$ , were determined. Criteria of the best fit were differential spectrum,  $\chi^2$ , and physical meaning of parameters. An instrumental (systematic) error for each spectrum point was ± 0.5 channel (the velocity scale), the instrumental (systematic) error for the hyperfine parameters was ± 1 channel. The relative instrumental error for  $A$  did not exceed 10 %. If an error calculated during the fit (fitting error) for these parameters exceeded the instrumental (systematic) error, we used the largest error. Values of  $\delta$  are given relative to  $\alpha$ -Fe at 295 K.

## Results and discussion

### Phase identification

Metallographic analysis (Fig. 1) of the iron meteorites slices showed that Anyujskij IIAB and Sikhote-Alin IIAB consist of  $\alpha$ -Fe(Ni,Co) with minor 'rhabdite' inclusions. In contrast, Aliskerovo IIIE-an and Sterlitamak IIIAB consist of  $\alpha$ -Fe(Ni,Co) and  $\gamma$ -Fe(Ni,Co) with plessite-textured  $\alpha$ -Fe(Ni,Co)/ $\alpha_2$ -Fe(Ni,Co) +  $\gamma$ -Fe(Ni,Co). Rims of  $\gamma$ -FeNi were observed in Aliskerovo IIIE-an. As for Dronino iron-ung meteorite, the duplex structure of  $\alpha$ -Fe(Ni,Co) and  $\alpha_2$ -Fe(Ni,Co) was observed (see also Grokhovsky *et al.*, 2005). The XRD study demonstrated

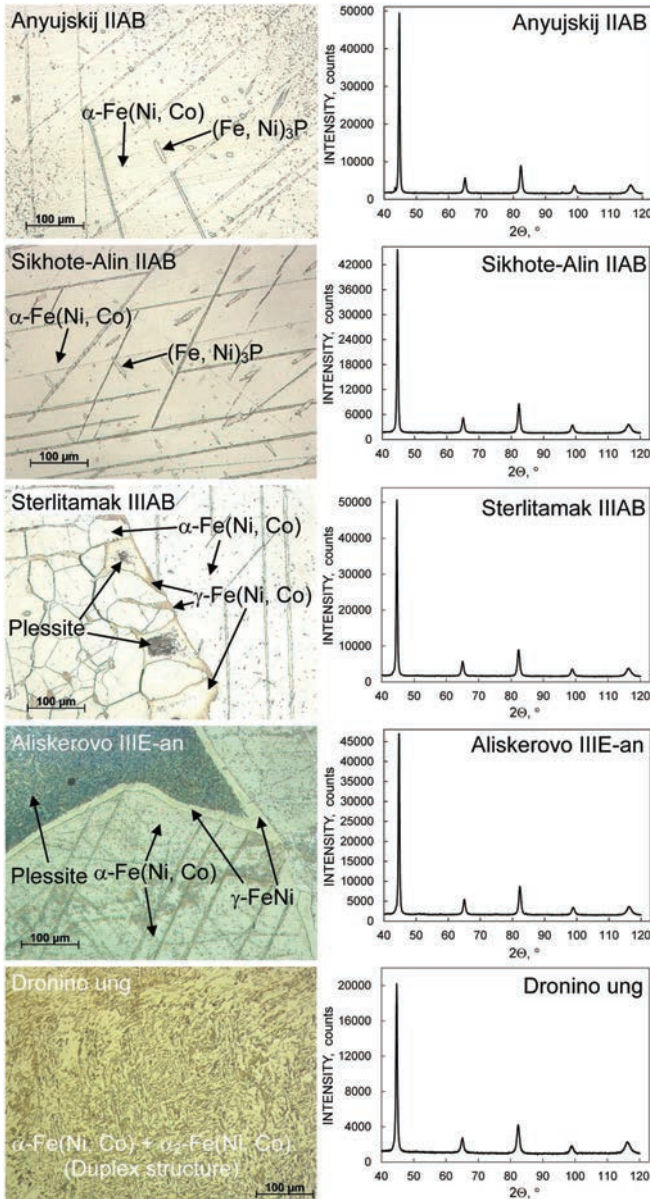


Fig. 1 Metallographic analysis of optical microphotographs and X-ray diffraction patterns for iron meteorites Anyujskij IIAB, Sikhote-Alin IIAB, Sterlitamak IIIAB, Aliskerovo IIIE-an and Dronino iron-ung. (online version in colour)

the presence of the main b.c.c. Fe-Ni-Co phase in all studied meteorites (Fig. 1). The XRD analysis of the weathering products showed some differences between studied samples (XRD patterns for the external surface oxidation products in Dronino fragment No 2 and for the external solid layer of a concretion found in the clay sand surrounding Dronino fragment No 1 are shown in Fig. 2). The internal surface oxidation layer from Dronino fragment No 1 contains magnetite/maghemite (XRD cannot distinguished these minerals well), goethite and probably small amounts of ferrihydrite, whereas the external surface oxidation layer from this fragment contains mainly goethite and probably ferrihydrite. In contrast, the

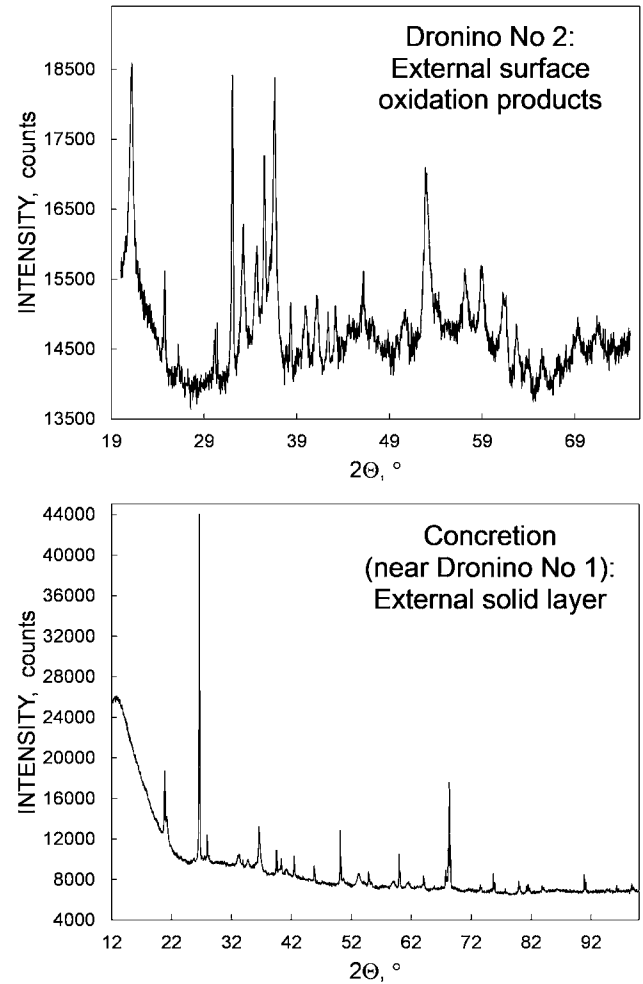


Fig. 2 X-ray diffraction patterns of the external surface oxidation products from Dronino meteorite fragment No 2 and external matter of concretion found in clay sand surrounding Dronino meteorite fragment No 1.

external surface oxidation layer from Dronino fragment No 2 demonstrates the presence of magnetite/maghemite, goethite, probably ferrihydrite and siderite. Both internal and external layers in the concretion consist of goethite and probably ferrihydrite.

### Mössbauer spectroscopy of the meteorite matrices

The Mössbauer spectra of iron meteorites measured at 295 K are shown in Fig. 3 in comparison with the spectrum of the standard absorber  $\alpha$ -Fe foil with a thickness of 7  $\mu\text{m}$ . All meteorites spectra demonstrate visually asymmetric six-line patterns with broader lines in comparison with the  $\alpha$ -Fe foil spectrum. This may indicate complex spectra of meteorites metal. The best fits of these spectra revealed different number of spectral components whose parameters are listed in Table 1. Basing on previous Mössbauer studies of b.c.c. Fe-Ni and Fe-Co alloys (Vincze *et al.*, 1974) and f.c.c. Fe-Ni alloys (Valderruten *et al.*, 2006) and iron meteorites (Scorzelli,

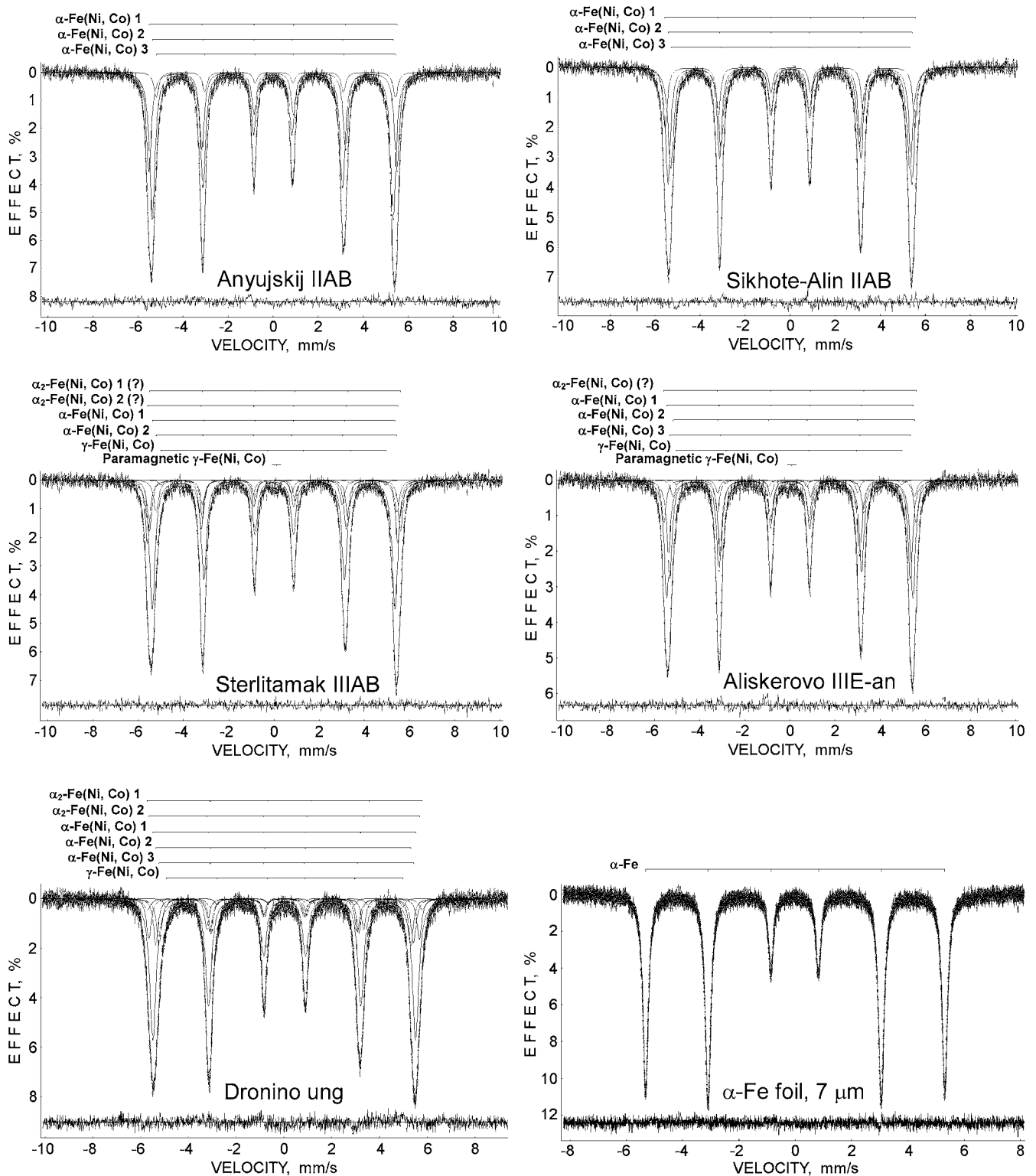


Fig. 3 Mössbauer spectra of iron meteorites Anyujskij IIAB, Sikhote-Alin IIAB, Sterlitamak IIIAB, Aliskerovo IIIE-an and Dronino iron-ung in comparison with the standard absorber  $\alpha$ -Fe foil with a thickness of 7  $\mu\text{m}$  measured at 295 K. Indicated spectral components are the results of the best fits. Differential spectra are shown below.

1991; Dos Santos *et al.*, 2015), we related the obtained Mössbauer hyperfine parameters of the spectral components to  $\alpha$ -Fe(Ni,Co),  $\alpha_2$ -Fe(Ni,Co) and  $\gamma$ -Fe(Ni,Co), as shown in Table 1 and in Fig. 3. The presence of several

spectral components related to the same mineral can be explained by different distributions of Ni and Co (concentration variations) within the same phase. The Mössbauer spectra of Anyujskij IIAB and Sikhote-Alin

Table 1. Mössbauer parameters of iron meteorites.

Sample	$\Gamma$ , mm/s	$\delta$ , mm/s	$\Delta E_Q$ , mm/s	$H_{\text{eff}}$ , kOe	A, %	Component <sup>a</sup>
Anyujskij IIAB	0.270 ± 0.040	0.010 ± 0.020	-0.037 ± 0.031	342.3 ± 0.6	36	$\alpha$ -Fe(Ni,Co) 1
	0.287 ± 0.040	-0.015 ± 0.020	-0.002 ± 0.032	332.5 ± 0.6	56	$\alpha$ -Fe(Ni,Co) 2
	0.255 ± 0.040	0.083 ± 0.020	0.082 ± 0.020	330.0 ± 0.8	8	$\alpha$ -Fe(Ni,Co) 3
Sikhote-Alin IIAB	0.240 ± 0.040	0.011 ± 0.020	-0.034 ± 0.020	345.1 ± 0.6	19	$\alpha$ -Fe(Ni,Co) 1
	0.265 ± 0.040	-0.004 ± 0.020	-0.010 ± 0.020	336.5 ± 0.6	40	$\alpha$ -Fe(Ni,Co) 2
	0.313 ± 0.040	-0.001 ± 0.020	0.014 ± 0.020	329.7 ± 0.6	41	$\alpha$ -Fe(Ni,Co) 3
Sterlitamak IIIAB	0.233 ± 0.040	0.057 ± 0.020	-0.007 ± 0.020	344.7 ± 0.6	16	$\alpha_2$ -Fe(Ni,Co) 1 (?)
	0.239 ± 0.040	-0.031 ± 0.020	-0.046 ± 0.020	343.7 ± 0.6	20	$\alpha_2$ -Fe(Ni,Co) 2 (?)
	0.295 ± 0.040	0.001 ± 0.020	-0.024 ± 0.020	333.4 ± 0.6	50	$\alpha$ -Fe(Ni,Co) 1
Aliskerovo IIIE-an	0.263 ± 0.040	0.024 ± 0.020	0.182 ± 0.020	330.7 ± 0.7	11	$\alpha$ -Fe(Ni,Co) 2
	0.238 ± 0.071	0.243 ± 0.020	-0.534 ± 0.041	309.1 ± 1.6	2	$\gamma$ -Fe(Ni,Co)
	0.352 ± 0.152	0.128 ± 0.050	-	-	1	Paramagnetic $\gamma$ -Fe(Ni,Co)
Dronino iron-ung	0.234 ± 0.040	0.015 ± 0.020	-0.024 ± 0.020	347.1 ± 0.6	14	$\alpha_2$ -Fe(Ni,Co) (?)
	0.269 ± 0.040	0.003 ± 0.020	-0.020 ± 0.020	338.6 ± 0.6	43	$\alpha$ -Fe(Ni,Co) 1
	0.233 ± 0.040	0.036 ± 0.020	0.274 ± 0.028	332.3 ± 1.1	5	$\alpha$ -Fe(Ni,Co) 2
Dronino iron-ung	0.259 ± 0.040	0.001 ± 0.020	0.003 ± 0.020	330.9 ± 0.6	35	$\alpha$ -Fe(Ni,Co) 3
	0.233 ± 0.096	0.006 ± 0.020	-0.096 ± 0.048	310.1 ± 2.1	2	$\gamma$ -Fe(Ni,Co)
	0.664 ± 0.246	0.071 ± 0.069	-	-	1	Paramagnetic $\gamma$ -Fe(Ni,Co)
Dronino iron-ung	0.329 ± 0.044	0.144 ± 0.014	-0.209 ± 0.024	357.1 ± 1.2	4	$\alpha_2$ -Fe(Ni,Co) 1
	0.238 ± 0.020	0.034 ± 0.010	-0.048 ± 0.010	351.5 ± 0.5	12	$\alpha_2$ -Fe(Ni,Co) 2
	0.322 ± 0.020	0.026 ± 0.010	-0.016 ± 0.010	341.3 ± 0.5	55	$\alpha$ -Fe(Ni,Co) 1
Dronino iron-ung	0.233 ± 0.020	0.013 ± 0.010	-0.062 ± 0.010	331.3 ± 0.5	13	$\alpha$ -Fe(Ni,Co) 2
	0.264 ± 0.020	0.048 ± 0.010	0.011 ± 0.010	330.4 ± 0.5	14	$\alpha$ -Fe(Ni,Co) 3
	0.233 ± 0.020	0.055 ± 0.010	-0.062 ± 0.019	307.8 ± 0.8	2	$\gamma$ -Fe(Ni,Co)

<sup>a</sup>Components correspond to spectral components indicated in Fig. 3.

IIAB meteorites consist of three spectral components with different values of  $H_{\text{eff}}$ , which were related to  $\alpha$ -Fe(Ni,Co) regions with local variations in Ni and Co concentration. However, the relative areas of these components were different for Anyujskij IIAB and Sikhote-Alin IIAB meteorites. The latter may be a result of different variation of Ni concentration in the  $\alpha$ -Fe(Ni,Co) regions in these meteorites. The Mössbauer spectra of Aliskerovo IIIE-an, Sterlitamak IIIAB and Dronino iron-ung showed the presence of more spectral components. Five magnetic components with different values of  $H_{\text{eff}}$  revealed from the spectra of Aliskerovo IIIE-an and Sterlitamak IIIAB may be related to the possible presence of  $\alpha_2$ -Fe(Ni,Co) as well as to  $\alpha$ -Fe(Ni,Co) and  $\gamma$ -Fe(Ni,Co). Mössbauer spectral components with the largest magnetic hyperfine fields obtained for two pairs of meteorites such as Anyujskij IIAB & Sikhote-Alin IIAB and Aliskerovo IIIE-an & Sterlitamak IIIAB have similar values of  $H_{\text{eff}}$  (Table 1). In case of Anyujskij IIAB and Sikhote-Alin IIAB these spectral components were assigned to  $\alpha$ -Fe(Ni,Co). However, in case of Aliskerovo IIIE-an and Sterlitamak IIIAB we can suggest that these magnetic components may be related to  $\alpha_2$ -Fe(Ni,Co) due to the presence of plessite structures in these meteorites (see Fig. 1) consisting of both  $\alpha$ -Fe(Ni,Co)/ $\alpha_2$ -Fe(Ni,Co) and  $\gamma$ -Fe(Ni,Co). The values of  $H_{\text{eff}}$  for  $\gamma$ -Fe(Ni,Co) are lower than those for  $\alpha$ -Fe(Ni,Co). It was interesting to observe a minor single peak component in the spectra of Aliskerovo IIIE-an and Sterlitamak IIIAB which could be related to paramagnetic  $\gamma$ -Fe(Ni,Co) with Ni concentration within the range of  $\sim 29$ – $33$  at.% (see Baldokhin *et al.*, 1999 and also Dunlap, 1997). Basing on Mössbauer results we can suggest different content of  $\alpha_2$ -Fe(Ni,Co) and  $\alpha$ -Fe(Ni,Co) in Aliskerovo IIIE-an and Sterlitamak IIIAB meteorites. Two magnetic sextets with the largest values of  $H_{\text{eff}}$  revealed in the Dronino iron-ung Mössbauer spectrum can be related to  $\alpha_2$ -Fe(Ni,Co) with some local variations in Ni content. Three magnetic sextets were associated with  $\alpha$ -Fe(Ni,Co) and one minor sextet with the smallest value of  $H_{\text{eff}}$  was assigned to  $\gamma$ -Fe(Ni,Co).

### Dronino meteorite weathering products

The Mössbauer spectra of surface weathering products of Dronino fragments are shown in Fig. 4. These spectra are very complex and contain magnetic sextets and paramagnetic quadrupole doublets. The results of the best fits of these spectra are shown in Fig. 4 and parameters are collected in Table 2. The spectrum of the internal surface oxidation products from Dronino fragment No 1 was decomposed into eleven components with eight magnetic and three paramagnetic subspectra. The magnetic components with the largest values of  $H_{\text{eff}}$  were assigned to magnetite and maghemite. This iron oxides have tetrahedral (A) and octahedral [B] position for iron cations. In case of magnetite  $\text{Fe}_3\text{O}_4$  there is an electron hopping between  $\text{Fe}^{2+}$  and  $\text{Fe}^{3+}$  in the [B] sites, that is why the values of  $\delta$  for the  $^{57}\text{Fe}$  in octahedral positions are larger

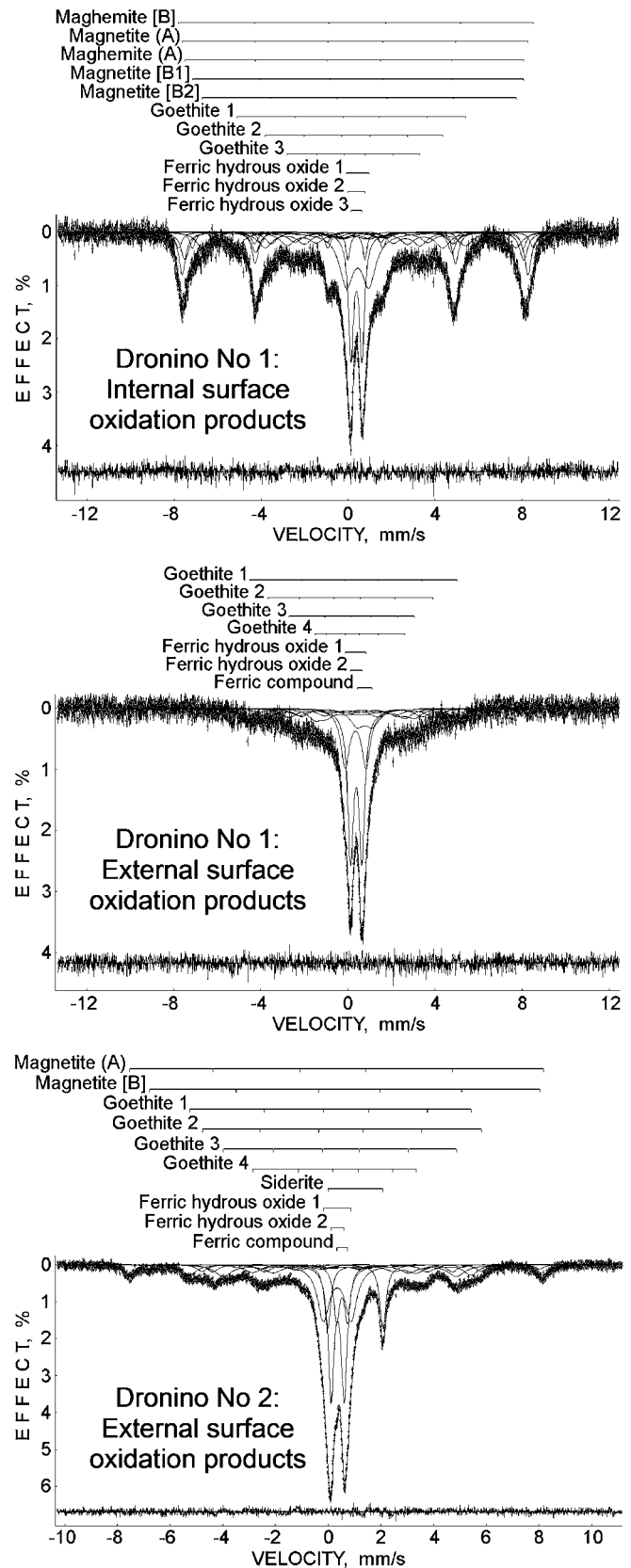


Fig. 4. Mössbauer spectra of the surface oxidation products from Dronino meteorite fragments No 1 and No 2 found in clay sand in different places. Indicated spectral components are the results of the best fits. Differential spectra are shown below.

Table 2. Mössbauer parameters of the Dronino surface oxidation products.

Sample	$\Gamma$ , mm/s	$\delta$ , mm/s	$\Delta E_Q$ , mm/s	$H_{\text{eff}}$ , kOe	A, %	Component <sup>a</sup>	
Dronino No 1 internal surface oxidation products	$0.363 \pm 0.073$	$0.397 \pm 0.015$	$-0.065 \pm 0.024$	$507.1 \pm 2.1$	5	Magnetite [B]	
	$0.376 \pm 0.036$	$0.332 \pm 0.013$	$-0.009 \pm 0.013$	$494.0 \pm 0.9$	13	Magnetite (A)	
	$0.449 \pm 0.047$	$0.277 \pm 0.017$	$0.029 \pm 0.027$	$483.9 \pm 1.9$	10	Magnetite (A)	
	$0.314 \pm 0.081$	$0.425 \pm 0.023$	$0.056 \pm 0.029$	$472.8 \pm 1.8$	4	Magnetite [B1]	
	$0.664 \pm 0.068$	$0.578 \pm 0.018$	$-0.146 \pm 0.035$	$449.0 \pm 1.9$	8	Magnetite [B2]	
	$0.776 \pm 0.070$	$0.380 \pm 0.021$	$-0.456 \pm 0.040$	$326.4 \pm 1.5$	9	Goethite 1	
	$0.776 \pm 0.026$	$0.316 \pm 0.019$	$-0.095 \pm 0.033$	$253.9 \pm 1.7$	10	Goethite 2	
	$0.776 \pm 0.026$	$0.286 \pm 0.025$	$-0.057 \pm 0.040$	$189.6 \pm 1.5$	8	Goethite 3	
	$0.776 \pm 0.026$	$0.444 \pm 0.013$	$1.033 \pm 0.019$	–	16	FeOOH 1	
	$0.233 \pm 0.026$	$0.389 \pm 0.013$	$0.782 \pm 0.014$	–	3	FeOOH 2	
	$0.284 \pm 0.026$	$0.390 \pm 0.013$	$0.503 \pm 0.013$	–	14	FeOOH 3	
	Dronino No 1 external surface oxidation products	$0.776 \pm 0.026$	$0.425 \pm 0.040$	$-0.344 \pm 0.071$	$297.3 \pm 1.9$	11	Goethite 1
		$0.776 \pm 0.026$	$0.104 \pm 0.048$	$-0.036 \pm 0.091$	$236.8 \pm 2.7$	10	Goethite 2 (?)
		$0.776 \pm 0.154$	$0.349 \pm 0.040$	$-0.303 \pm 0.076$	$177.8 \pm 2.8$	10	Goethite 3
		$0.776 \pm 0.026$	$0.442 \pm 0.051$	$0.270 \pm 0.082$	$126.5 \pm 3.7$	9	Goethite 4
		$0.423 \pm 0.034$	$0.322 \pm 0.013$	$0.926 \pm 0.027$	–	14	FeOOH 1
$0.300 \pm 0.026$		$0.379 \pm 0.013$	$0.514 \pm 0.013$	–	28	FeOOH 2	
$0.767 \pm 0.106$		$0.604 \pm 0.032$	$0.750 \pm 0.028$	–	18	Fe <sup>3+</sup> compound	
$0.474 \pm 0.028$		$0.245 \pm 0.011$	$0.154 \pm 0.021$	$487.6 \pm 0.6$	7	Magnetite (A)	
$0.399 \pm 0.063$		$0.708 \pm 0.021$	$-0.167 \pm 0.042$	$459.3 \pm 1.3$	2	Magnetite [B]	
$0.628 \pm 0.050$		$0.375 \pm 0.014$	$-0.592 \pm 0.038$	$331.5 \pm 0.8$	8	Goethite 1	
Dronino No 2 external surface oxidation products	$0.495 \pm 0.077$	$0.500 \pm 0.022$	$0.030 \pm 0.043$	$329.3 \pm 1.2$	4	Goethite 2	
	$0.776 \pm 0.044$	$0.462 \pm 0.012$	$-0.040 \pm 0.022$	$274.8 \pm 1.2$	11	Goethite 3	
	$0.776 \pm 0.067$	$0.444 \pm 0.021$	$-0.427 \pm 0.033$	$192.7 \pm 1.2$	7	Goethite 4	
	$0.286 \pm 0.022$	$1.031 \pm 0.011$	$2.100 \pm 0.011$	–	11	Siderite	
	$0.549 \pm 0.022$	$0.343 \pm 0.011$	$1.044 \pm 0.011$	–	18	FeOOH 1	
	$0.260 \pm 0.022$	$0.358 \pm 0.011$	$0.496 \pm 0.011$	–	21	FeOOH 2	
	$0.274 \pm 0.022$	$0.527 \pm 0.011$	$0.411 \pm 0.011$	–	9	Fe <sup>3+</sup> compound	

<sup>a</sup>Components correspond to spectral components indicated in Fig. 4.

than those for (A) positions reflecting effective  $\text{Fe}^{2.5+}$  charge, while in the case of maghemite  $\gamma\text{-Fe}_2\text{O}_3$  there is no such electron hopping and the values of  $\delta$  for the  $^{57}\text{Fe}$  in tetrahedral and octahedral positions have no so significant difference. The values of  $H_{\text{eff}}$  for the (A) sites in maghemite are larger than those for the [B] sites while in magnetite there is inverse difference of  $H_{\text{eff}}$  for the  $^{57}\text{Fe}$  in the (A) and [B] sites (*e.g.*, Goodman, 1994; Murad, 2010). Therefore, it was possible to distinguish spectral components related to maghemite and magnetite (see Table 2). It should be noted that two magnetic components were related to the [B1] and [B2] sites in magnetite. This may be possible taking into account the presence of Ni in the oxidized metal alloy. Therefore, formation of magnetite with some substitution of Fe cations by  $\text{Ni}^{2+}$  ions, which preferably occupy the [B] sites in the inverse  $\text{NiFe}_2\text{O}_4$  spinel, may be possible. Oshtrakh *et al.* (2013b) showed that the distribution of probability of different numbers of  $\text{Ni}^{2+}$  ions in the local environment of the  $^{57}\text{Fe}$  in the (A) and [B] sites in  $\text{NiFe}_2\text{O}_4$  leads to the appearance of different magnetic sextets related to these sites. Therefore, the presence of two sextets assigned to the [B1] and [B2] sites can reflect incorporation of some  $\text{Ni}^{2+}$  ions into magnetite with some distortion of the part of the [B] sites. Other magnetic components could be associated with small goethite particles with different sizes influencing the values of  $H_{\text{eff}}$ . Three quadrupole doublets could be related to ferric hydrous oxides with a Néel temperature below 300 K, or to nanosized goethite particles in the superparamagnetic state. There are three ferric hydrous oxides, ferrihydrite, akaganéite and lepidocrocite, which are paramagnetic at room temperature. The presence of ferrihydrite may be considered as the most likely, however, this suggestion needs further evidence. Therefore, we assigned these quadrupole doublets to ferric hydrous oxides in general.

It was interesting to observe differences in the weathering products in the external surface layers of two Dronino fragments No 1 and No 2 found in different places. Components revealed in the Mössbauer spectrum of the external surface oxidation products from fragment No 1 were related to goethite (magnetic sextets) and other ferric hydrous oxides (paramagnetic quadrupole doublets). One quadrupole doublet with hyperfine parameters related to ferric high spin compound was not identified yet. In contrast, it was possible to observe two magnetic sextets associated with the (A) and [B] sites in magnetite and four magnetic sextets assigned to goethite particles with different sizes in the Mössbauer spectrum of the external surface oxidation products from fragment No 2. Moreover, a new quadrupole doublet with hyperfine parameters corresponding to ferrous compound was found in addition to paramagnetic quadrupole doublets related to ferric hydrous oxides and an unidentified ferric compound. These parameters appeared to be close to siderite (see Dideriksen *et al.*, 2015), which was in agreement with the XRD results for these oxidation products. Formation of siderite in the surface weathered layer of

Dronino fragment No 2 may be a result of bioreduction of goethite in clay sand (Maitte *et al.*, 2015).

### The concretion in clay sand surrounding Dronino

Various ferric hydrous oxides formed during the Dronino iron weathering in clay sand could diffuse into the clay and be transferred with surrounding water. In this respect, the concretion formed in the clay sand surrounding Dronino fragment No 1 is interesting. The Mössbauer spectra of internal friable and external solid layers of this concretion are shown in Fig. 5. Although these spectra shapes look different, the best fits of Mössbauer spectra demonstrated the same spectral components: magnetic sextets related to goethite particles with different sizes, and paramagnetic quadrupole doublets associated with ferric hydrous oxides (parameters are given in Table 3). The main differences are related to the range of the  $H_{\text{eff}}$  values for magnetic components for two concretion samples and their relative

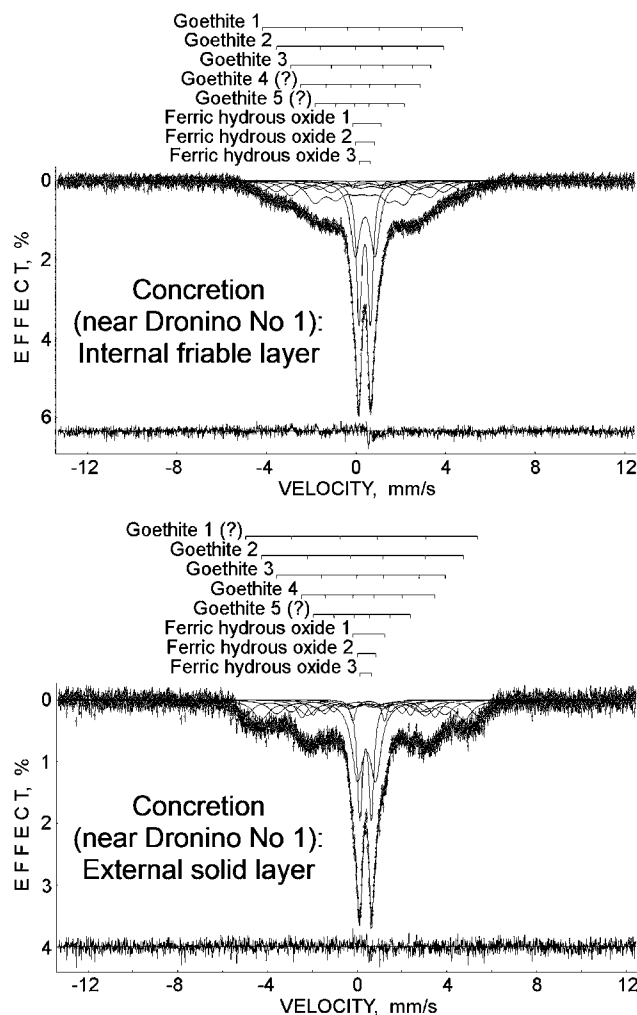


Fig. 5. Mössbauer spectra measured at 295 K of the internal and external layers of a concretion found in the clay sand surrounding Dronino fragment No 1. Indicated spectral components are the results of the best fits. Differential spectra are shown below.



Table 3. Mössbauer parameters of concretion matter found in the clay sand surrounding Dronino fragment No 1.

Sample	$\Gamma$ , mm/s	$\delta$ , mm/s	$\Delta E_Q$ , mm/s	$H_{\text{eff}}$ , kOe	$A$ , %	Component <sup>a</sup>	
Internal friable layer	$0.834 \pm 0.078$	$0.302 \pm 0.030$	$-0.044 \pm 0.055$	$277.1 \pm 1.5$	10	Goethite 1	
	$0.833 \pm 0.061$	$0.366 \pm 0.027$	$-0.392 \pm 0.053$	$232.4 \pm 2.1$	10	Goethite 2	
	$0.834 \pm 0.141$	$0.454 \pm 0.018$	$-0.485 \pm 0.031$	$193.7 \pm 2.4$	14	Goethite 3	
	$0.488 \pm 0.310$	$0.199 \pm 0.055$	$0.004 \pm 0.109$	$165.8 \pm 5.2$	2	Goethite 4 (?)	
	$0.833 \pm 0.061$	$0.209 \pm 0.017$	$-0.103 \pm 0.035$	$124.4 \pm 1.4$	20	Goethite 5 (?)	
	$0.233 \pm 0.092$	$0.485 \pm 0.018$	$1.267 \pm 0.035$	–	1	FeOOH 1	
	$0.517 \pm 0.026$	$0.408 \pm 0.013$	$0.879 \pm 0.015$	–	21	FeOOH 2	
	$0.283 \pm 0.028$	$0.391 \pm 0.026$	$0.511 \pm 0.013$	–	22	FeOOH 3	
	External solid layer	$0.748 \pm 0.067$	$0.137 \pm 0.029$	$0.132 \pm 0.056$	$321.7 \pm 1.6$	13	Goethite 1 (?)
		$0.834 \pm 0.026$	$0.327 \pm 0.019$	$-0.173 \pm 0.027$	$281.1 \pm 1.7$	17	Goethite 2
$0.834 \pm 0.026$		$0.382 \pm 0.029$	$-0.425 \pm 0.052$	$233.7 \pm 2.3$	12	Goethite 3	
$0.559 \pm 0.066$		$0.395 \pm 0.018$	$0.223 \pm 0.034$	$184.6 \pm 1.3$	10	Goethite 4	
$0.470 \pm 0.055$		$0.213 \pm 0.019$	$-0.007 \pm 0.027$	$135.2 \pm 1.2$	7	Goethite 5 (?)	
$0.294 \pm 0.048$		$0.521 \pm 0.013$	$1.425 \pm 0.022$	–	3	FeOOH 1	
$0.600 \pm 0.030$		$0.422 \pm 0.013$	$0.812 \pm 0.024$	–	22	FeOOH 2	
$0.271 \pm 0.026$		$0.383 \pm 0.013$	$0.517 \pm 0.013$	–	16	FeOOH 3	

<sup>a</sup>Components correspond to spectral components indicated in Fig. 5.

areas. This difference can be explained as a result of the formation of larger goethite particles in the external solid layer with probably a higher degree of crystallinity, whereas goethite particles are smaller with a more disordered structure in the internal friable layer.

## Conclusion

The study of five iron meteorites Anyujskij IIAB, Sikhote-Alin IIAB (both are coarse octahedrites), Sterlitamak IIIAB, Aliskerovo IIIE-an (both are medium octahedrites) and Dronino iron-ung (probably an ataxite) demonstrated different complexity of the Mössbauer spectra related to different phase composition of the metallic matrix. Anyujskij IIAB and Sikhote-Alin IIAB consist of  $\alpha$ -Fe(Ni,Co) only (as the main metallic mineral detected by Mössbauer spectroscopy) while Sterlitamak IIIAB, Aliskerovo IIIE-an and Dronino iron-ung meteorites consist of  $\alpha$ -Fe(Ni,Co),  $\alpha_2$ -Fe(Ni,Co) and  $\gamma$ -Fe(Ni,Co) in different quantities. Variations in the Mössbauer hyperfine parameters for the same phases were explained as a result of different local variations in Ni and Co concentration in the <sup>57</sup>Fe local microenvironment and reflected by the hyperfine parameters.

An analysis of Dronino iron-ung metal weathering in clay sand (fragment No 1) demonstrated that in the internal oxidation layer there is formation of magnetite and maghemite with further transformation into goethite and other ferric hydrous oxides. The composition of the external oxidation layer was different for two Dronino fragments (No 1 and No 2) found in different places. In case of fragment No 1 this layer consists of goethite and other ferric hydrous oxides mainly, whereas that of fragment No 2 additionally contains magnetite and siderite (the latter can be considered as a product of bacterial reduction of goethite). The composition of concretion found in the clay sand surrounding fragment No 1 is the same in the

internal and external layers (goethite and other ferric hydrous oxides) with different goethite particle size and degree of crystallinity in these layers.

**Acknowledgements:** This work was supported in part by the Ministry of Education and Science of Russian Federation (basic financing for the Projects # 2085 and # 1514) and by Act 211 Government of the Russian Federation, contract No 02.A03.21.0006.

## References

- Baldokhin, Yu.V., Tcherdyntsev, V.V., Kaloshkin, S.D., Kochetov, G.A., Pustov, Yu.A. (1999): Transformations and fine magnetic structure of mechanically alloyed Fe–Ni alloys. *J. Mag. Mag. Mater.*, **203**, 313–315.
- Buchwald, V.F. (1975): Handbook of iron meteorites. University of California Press, Berkeley, 1418 p.
- Dideriksen, K., Frandsen, C., Bovet, N., Wallace, A.F., Sel, O., Arbour, T., Navrotsky, A., De Yoreo, J.J., Banfield, J.F. (2015): Formation and transformation of a short range ordered iron carbonate precursor. *Geochim. Cosmochim. Acta*, **164**, 94–109.
- Dos Santos, E., Gattacceca, J., Rochette, P., Scorzelli, R.B., Fillion, G. (2015): Magnetic hysteresis properties and <sup>57</sup>Fe Mössbauer spectroscopy of iron and stony-iron meteorites: Implications for mineralogy and thermal history. *Phys. Earth Planet. Inter.*, **242**, 50–64.
- Dunlap, R.A. (1997): A Mössbauer effect investigation of the enstatite chondrite from Abeo, Canada. *Hyperfine Interact.*, **110**, 209–215.
- Goldstein, J.I., Scott, E.R.D., Chabot, N.L. (2009): Iron meteorites: crystallization, thermal history, parent bodies, and origin. *Chem. Erde.*, **69**, 293–325.
- Goodman, B.A. (1994): in “Clay mineralogy: spectroscopic and chemical determinative methods”, ed. Wilson, M.J. Chapman & Hall, London, 68–119.

- Grady, M., Pratesi, G., Moggi Cecchi, V. (2014): Atlas of meteorites. Cambridge University Press, Cambridge, 384 p.
- Grokhovsky, V.I., Oshtrakh, M.I., Milder, O.B., Semionkin, V.A. (2005): Mössbauer spectroscopy of iron meteorite dronino and products of its corrosion. *Hyperfine Interact.*, **166**, 671–677.
- Grokhovsky, V.I., Zhiganova, E.V., Larionov, M.Yu., Uimina, K. A., Oshtrakh, M.I. (2008): Mössbauer spectroscopy with high velocity resolution in the meteorites study. *The Phys. Metals Metallogr.*, **105**, 177–187.
- Grokhovsky, V.I., Oshtrakh, M.I., Petrova, E.V., Larionov, M.Yu., Uymina, K.A., Semionkin, V.A. (2009): Mössbauer spectroscopy with high velocity resolution in the study of iron-bearing minerals in meteorites. *Eur. J. Mineral.*, **21**, 51–63.
- Maitte, B., Jorand, F.P.A., Grgic, D., Abdelmoula, M., Carteret, C. (2015): Remineralization of ferrous carbonate from bioreduction of natural goethite in the Lorraine iron ore (Minette) by *Shewanella putrefaciens*. *Chem. Geol.*, **412**, 48–58.
- Murad, E. (2010): Mössbauer spectroscopy of clays, soils and their mineral constituents. *Clay Mineral.*, **45**, 413–430.
- Oshtrakh, M.I. & Semionkin, V.A. (2013): Mössbauer spectroscopy with a high velocity resolution: advances in biomedical, pharmaceutical, cosmochemical and nanotechnological research. *Spectrochim. Acta, Part A: Molec. Biomolec. Spectroscopy*, **100**, 78–87.
- Oshtrakh, M.I., Grokhovsky, V.I., Petrova, E.V., Larionov, M.Yu., Uymina, K.A., Semionkin, V.A., Abramova, N.V. (2008): Study of meteorites using Mössbauer spectroscopy with high velocity resolution. in “Proceedings of the international conference “Mössbauer Spectroscopy in Materials Science 2008”, eds. M. Mashlan, R. Zboril. AIP Conference Proceedings, Melville, New York, **1070**, 131–139.
- Oshtrakh, M.I., Semionkin, V.A., Milder, O.B., Novikov, E.G. (2009): Mössbauer spectroscopy with high velocity resolution: an increase of analytical possibilities in biomedical research. *J. Radioanal. Nucl. Chem.*, **281**, 63–67.
- Oshtrakh, M.I., Grokhovsky, V.I., Petrova, E.V., Larionov, M.Yu., Goryunov, M.V., Semionkin, V.A. (2013a): Mössbauer spectroscopy with a high velocity resolution applied for the study of meteoritic iron-bearing minerals. *J. Mol. Struct.*, **1044**, 268–278.
- Oshtrakh, M.I., Ushakov, M.V., Senthilkumar, B., Kalai Selvan, R., Sanjeeviraja, C., Felner, I., Semionkin, V.A. (2013b): Study of NiFe<sub>2</sub>O<sub>4</sub> Nanoparticles Using Mössbauer Spectroscopy with a High Velocity Resolution. *Hyperfine Interact.*, **219**, 7–12.
- Oshtrakh, M.I., Maksimova, A.A., Goryunov, M.V., Yakovlev, G.A., Petrova, E.V., Larionov, M.Yu., Grokhovsky, V.I., Semionkin, V. A. (2015): Mössbauer spectroscopy with a high velocity resolution: advances in the study of meteoritic iron-bearing minerals. Proceedings of the Workshop on The Modern Analytical Methods Applied to Earth and Planetary Sciences. Ed. A. Gucsik. The MicroMatLab Kft Hungary, Sopron, 43–86.
- Rubin, A.E. (1997): Mineralogy of meteorite groups. *Meteor. Planet. Sci.*, **32**, 231–247.
- Scorzelli, R.B. (1991): Application of the Mössbauer effect to the study of meteorites - a review. *Hyperfine Interact.*, **66**, 249–258.
- Semionkin, V.A., Oshtrakh, M.I., Milder, O.B., Novikov, E.G. (2010): A high velocity resolution Mössbauer spectrometric system for biomedical research. *Bull. Rus. Acad. Sci.: Phys.*, **74**, 416–420.
- Valderruten, J.F., Alcazar, G.A.P., Greneche, J.M. (2006): Study of Fe–Ni alloys produced by mechanical alloying. *Phys., B: Cond. Mat.*, **384**, 316–318.
- Vincze, I., Campbell, I.A., Meyer, A.J. (1974): Hyperfine field and magnetic moments in b.c.c. Fe–Co and Fe–Ni. *Solid State Commun.*, **15**, 1495–1499.

Received 13 November 2015

Modified version received 31 January 2016

Accepted 4 April 2016